J. Basic. Appl. Sci. Res., 7(1)17-35, 2017
© 2017, TextRoad Publication
ISSN 2090-4304
Journal of Basic and Applied Scientific Research
www.textroad.com

Experimental and Numerical Investigation of Impingement Cooling of Gas Turbine Combustion Chamber Liner

Arkan Al Taie[1] and Hussain S. Abd[2]

University of Technology, Baghdad-Iraq

Received: August 12, 2016
Accepted: November 29, 2016

ABSTRACT

The field that relates with the combustor material development or liner cooling improvement has been attracted the engineers due to increase the power and the combustor life. The main task of this research is employing the ribs as a square shape to inspect the cooling improvement. In order to increase the wall cooling effectiveness as well as investigate the enhancement of impingement cooling, a square ribbed target surface (lateral arrangement) has been proposed. The main idea of the proposed method is to punched 36 holes with diameter of 5mm for each one and arrange it in inline array. The distance between jet to jet was 4 times of the jet hole diameter. 5000 to 15000 has been selected as a Reynolds numbers ranges while, height to diameter ratio of jets which represents the space between the jet and target plates are 2 and 3 times from the hole diameter. Two models of target plates models have been utilized which are, a clean target plate surface that represents the base line case model while, a second model was a lateral target surface with square ribs arrayed as rows at 45^0. Then, average wall cooling effectiveness estimation and Nusselt numbers calculated for each model. As a result, the second model proved superior on the first model at same conditions (Reynolds number and $\frac{H}{D}$) to enhance the Nusselt numbers and wall cooling effectiveness. Where, the enhancement percentages were 32.885%, 22.13% at $\frac{H}{D} = 2$ and 31.37%, 14.58% at $\frac{H}{D} = 3$ for Nusselt numbers and the wall cooling effectiveness, respectively. The numerical solution will be conducted to predict the flow pattern by using commercial CFD code (ANSYS FLUENT 14.5 package). Finally, the ribs leaded to reduce the temperature of combustor liner as well as increasing its life.

KEYWORDS: jet impingement, gas turbine, square ribbed target, lateral ribs, Impingement Cooling, Combustion Chamber Liner.

Nomenclature

A = Target plate surface area, m^2
A_h= Hole cross-sectional area, m^2
C_D= Discharge coefficient.
D = Jet hole diameter, m
H = Jet to target spacing, m
h_{av} = Averaged heat transfer coefficient, $W/m^2.k$
k = Thermal conductivity of the target plate, W/m.K
$\dot{m}$= Mass flow rate, kg/s
Nu= Nusselt number
$\overline{Nu}$ = Area-averaged Nusselt number
Q = Heat flow rate, Watt
Re = Reynolds number
S= Jet to jet spacing, m
t= thickness, m
T= Temperature, degree centigrade
Tw= Wall temperature, degree centigrade
X = Local length of the target plate, m
$\overline{\eta}$ = Average wall cooling effectiveness
ΔP = Change in pressure, N/m^2
ρ = Density of the air, kg/m^3

Subscript

s = crossflow
av.= average
in = inner target surface
j= jet
out = outer target surface
∞ = mainstream flow

Corresponding Author: Hussain S. Abd, University of Technology, Baghdad-Iraq.
E-Mail: hussainsaad1983@gmail .com

INTRODUCTION

Gas turbine combustors are also cooled by impinging air jets and there is increasing industrial interest to perfect the application for the cooling of combustor wall because it promises superior effectiveness over the conventional methods such as convective film and effusion cooling. The necessity for more effective combustor wall cooling arises from the desire to obtain higher operating temperature in the gas turbine cycle for increased work per unit of mass throughput as well as better efficiency. This will lead to lighter engines and higher capacity turbines. Unfortunately, the practical limit to cycle temperature is fixed by the material of the combustor. Many investigators have worked on impingement heat transfer. Earlier workers were more concerned with studies related to the use for heating and drying as applied in the paper and glass industries. Later workers have included other applications such as turbine blade cooling and combustor wall cooling. Some investigators worked with single rows of round and slot jets and some with multiple jet arrays. In comparing previous work of the authors with the present work, two significant problems were encountered. Firstly, some workers had defined a heat transfer coefficient in terms of a temperature difference between the impingement jet outlet and the target plate whereas other workers had used a temperature difference between the coolant supply temperature and the target plate. In the present work, the significance of these differences is assessed. Secondly, many other workers had used impingement geometries with significant cross flow in the impingement gap. The significant of the cross flow influences in the present work is assessed by investigating spatial temperature distributions on the impingement plate. Due to complexity of impinging jet structures in actual arrays, researchers have systematically studied the effects of geometrical parameters on heat transfer characteristics of impinging jets. Dano, Betrand, et-al**[1]** researched on the effects of nozzle geometry on the flow characteristics and the heat transfer performance. San and lai **[2]** studied the effect of jet-to-jet impingement spacing on heat transfer in staggered arrays. Cheong and Ireland **[3]** experimentally measured local heat transfer coefficient under an impinged jet with low nozzle-to-plate, z/d spacing. Several others have studied the effect of cross flow on jet structure and heat transfer including Florsguetz**[4]**, Kercher and Tabakoff**[5]**. Both Florschuets, and Kercher and Tabakoff developed correlations topredict the effects of cross flow on jet impingement heat transfer for inline and staggered arrays which are still used today in jet impingement research. Bailey and Bunker**[6]** studied the effect of sparse and dense arrays for large number of jets. Herbert and Ekkad**[7]**, investigated the effect of a stream wise pressure gradient for an inline array of sparse and dense configurations. As more information on geometrical parameters and their effect on impinging jets became available, othersstudied ways of increasing the jet effectiveness through target surface modification. Surface geometrics such as trip strips, protrusions or dimples can significantly alter the jet structure and potentially provide enhanced heat transfer. Ekkad and Kontrovitz**[8]** used a dimpled target surface. This concept proved inadequate in heat transfer enhancement and actually showed a drop in performance. Another concept employed in many internal cooling configuration is trip strips. Small strip placed on the surface break down boundary layers, increase local turbulence levels, and enhance heat transfer. The use of trip strips was studied in detail by Han et al **[9]** for internal channel flow, and later by Herbert and Ekkad**[10]** in jet impingement configurations .Andrews, Hussain and Ojobor S.N**[11]**, obtained full coverage impingement Heat Transfer, the influence of impingement jet size and correlated their result as h=460*(z/d)-0.15* G0.8.However, Hollworth and Berry **[12]** obtained a test rig with single sided air exit so that there was always an influence of cross flow. Secondly, the method of calculating the heat transfer coefficient using a long-mean of the temperature differences between the impingement plate and the plenum chamber air temperature was studied. This was an attempt to use a coolant temperature close to a jet outlet temperature. Hollworth and Berry also recognized this problem and they used a coolant temperature which was the average of the plenum temperature and jet outlet temperature. Thereafter, many other workers have used the plenum chamber temperature as the coolant. As the temperature differences between the coolant and the impingement plate varies with the coolant flow rate, the present method of evaluating *h* could give a slightly different value for *y* than using the plenum chamber temperature. This value of *y* is a function of *z/d* In this present work - impingement of air cooling on a hot plate of varied flow rate of air, was studied on a hot target plate. The influence of temperature difference and quality of heat input were considered for values of *h*, these however, were correlated with Reynolds number, Nusselt number, Prandtl number and coolant flow per unit surface area to show influence with *Nu* values.

The aim of present work

The purpose of present study is to estimate experimentally the heat transfer characteristics of multiple jets system impinged a ribbed flat target. A triangular ribs is used to represent the ribbed target surface. Two types of target plate are examined experimentally.

Experimental Set-up and Procedures

Experimental test rig and set-up

All experiments were carried out in a low-speed air flowing system is designed and constructed at the University of Technology-Mechanical Engineering Department.

Figure (1) shows the test rig schematic diagram and dimensions and photography. The air of the mainstream is drawn by a (2.5 kW) electrical blower (M) running with 2800 rpm. Main airspeed in the test section (E) is controlled by manually partially open gate and measured velocity by pitot tube that designed according to British standard (F) to maintain (20 m/s) through the test. The mainstreams temperature is flowing through settling chamber (H). In order to allow the air to reach the desired temperature ($40C^{o}$), it is initially routed out away from the test section by using a by-bass gate passage until maintaining the desired temperature.

The secondary flow(the jets crossflow)is regarded as the hot air of the heat transfer process, while the main stream flow is regarded as a cool air to save energy. The jets crossflow is drawn, by (3.0 kW) air pressure blower (A),to the plenum (D). The crossflow flow rate is measuered by using orifice meter (B) located at the crossflow piping system. The crossflow is heated (100C) by using an electrical heater (C). Both mainstream air and secondary flow are discharged through sigle exit (L) and their temperatures are measured befor get mixed at the test rig exit.

Fig. 1-a : Photography of the experimental test rig

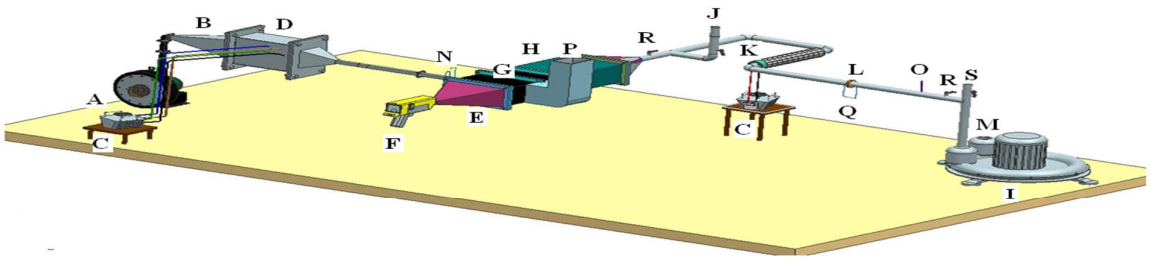

A. Air blower (Mainstream flow)
B. Diffuser
C. Variac
D. Settling chamber
E. Camera window
F. Infrared camera
G. Test section
H. Plenum
S. Injection side
Q. Manometer
I. Air blower (Secondary flow)
J. Transition line
K. Air heater
L. Orifice meter
M. Suction side
N. Pitot tube with manometer
O. Digital thermometer
P. Exhaust duct
R. Ball valve

Fig. 1-b :schematic of the experimental test rig
Fig. 1: Experimental test rig

Both air stream temperatures are obtained by digital electronic reader type (TM-903A) with the aid of thermocouples (type-K)at the test section. The cross flow temperature is taken at one chosen hole, since the pre-testing showed that all jet holes are indicated the same flow rate and temperature conditions. Thermography Infrared camera (Fluke Ti32), (N), is measured the thermal energy emitted from the backside target plate by the resistive air film as a temperature distribution through camera window (K).

Boundary condition

The mainstream flow physical variables are fixed at (V_∞ = 20 m/s) and (T_∞= 40 ^{0}C), and the secondary flow is at (T_s=100 ^{0}C) with varied mass flow rate according to the required Reynolds number. The flow is assumed to be turbulent.

Test section and test models

Figure (2) shows the test section 3-D schematic diagram of test rig assembly. Figure (3) shows the schematic diagram of the jet plat geometry and dimensions. Figure (4) shows the ribbed target plats for two models (a and b).

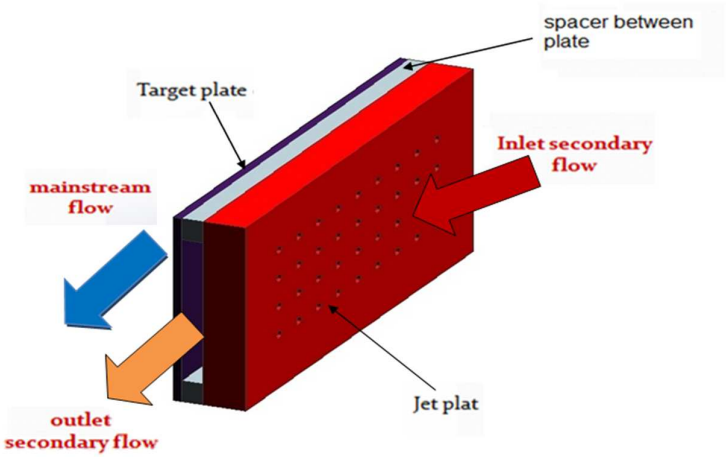

Fig. 2-a: Test section

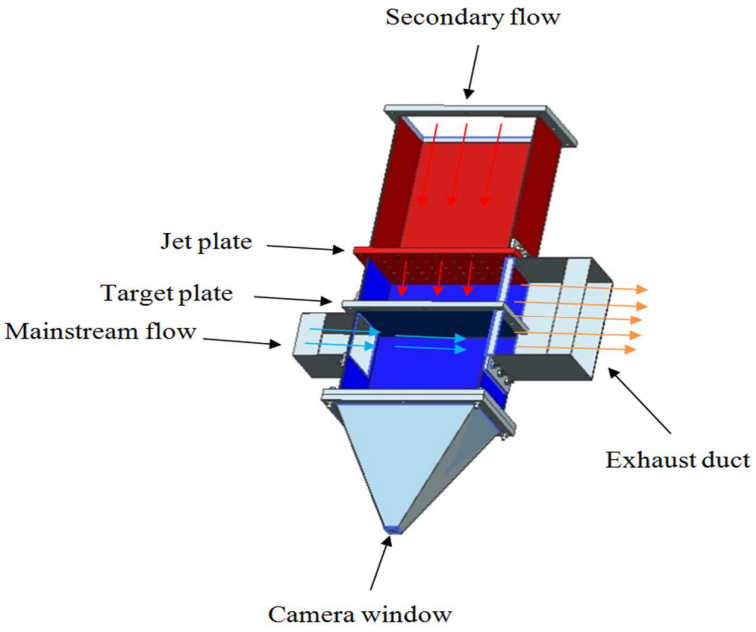

Fig. 2-b: Mechanzism Test section
Fig. 2: Test section

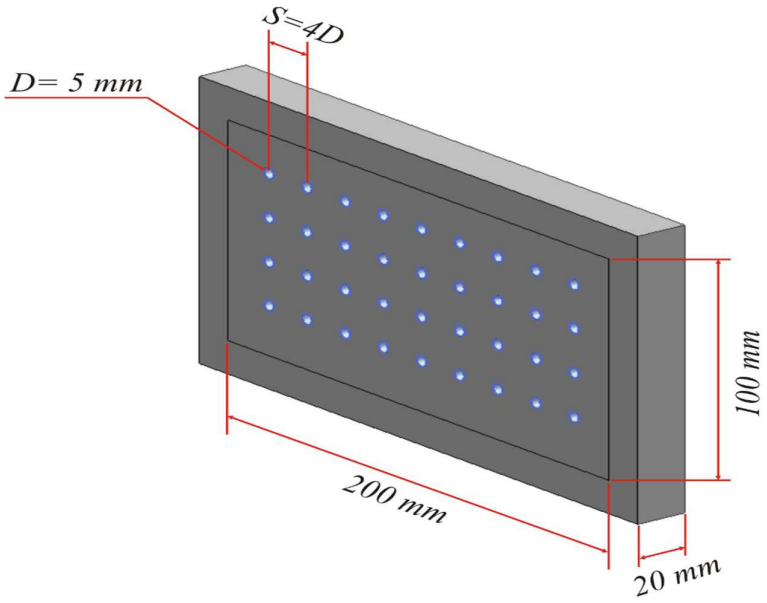

Fig. 3: Jet plate dimension

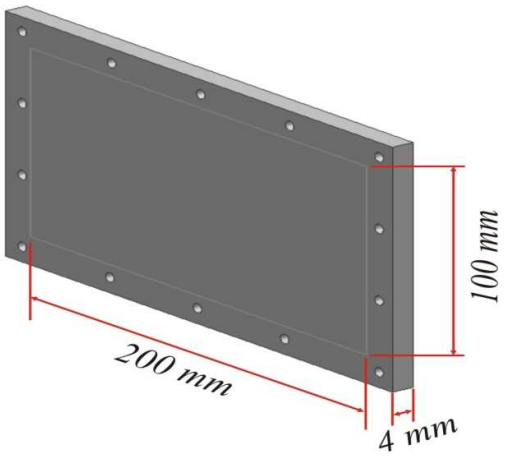

Fig. 4-a **:**Smoth Target plate

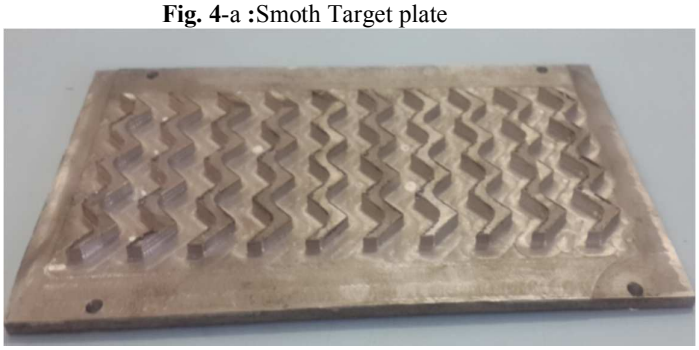

Fig. 4-b **:**Rib target plate(square ribbed)
Fig. 4: Target plates model

The calculations

Experimetal procedure calculation to estimate the averageheat transfer coefficeintcan be done as follows, the total heat lost from the impinging jets flow by mainstream flow can be calculated as follows:

$$Q_L = m \cdot C_p \Delta T = KA \frac{\Delta T_{av.}}{t} = havA(T_j \_ (Tw_{in})_{av}) \quad (1)$$

Where,

$$\Delta T_{av} = ((Tw_{in})_{av.} - (Tw_{out})_{av.}). \quad (2)$$

Then

$$(Tw_{in})_{av.} = \frac{Q_L * t}{KA} + (Tw_{out})_{av.} \quad (3)$$

where,

$$h_{av} = \frac{Q_L}{A\,(T_j - Tw_{in})} \quad (4)$$

Therefore, the average Nusselt number ($\overline{Nu}$) obtained is:

$$\overline{Nu} = \frac{\bar{h}D}{K_{air}} \quad (5)$$

The non-dimensional wall cooling effectiveness is defined as:

$$\bar{\eta} = \frac{T_\infty - Tw_{out}}{T_\infty - T_S} \quad (6)$$

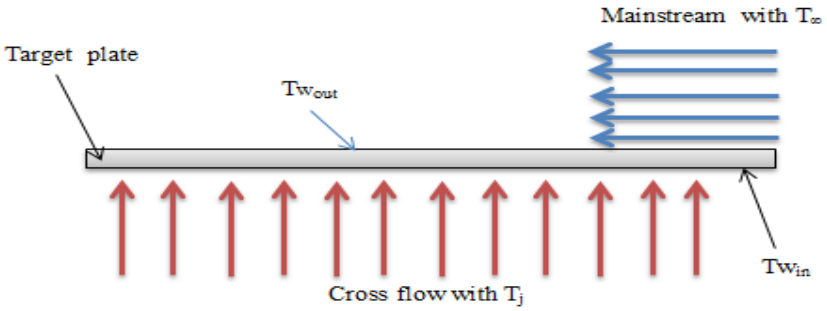

Fig. 5: Target plate with cross flow and mainstream

Discharge Coefficient Evaluation (C_D)

The flow velocity and the geometrical parameters on the discharge coefficient can be calculated, the pressure losses at the impingement side are defined by the non-dimensional discharge coefficient as:

$$\Delta P = \frac{m_h{}^2}{2\, A_h{}^2 C D^2\, \rho} \qquad (7)$$

Therefore,

$$C_D = \frac{m_h}{A_h \sqrt{2\, \rho\, \Delta P}} \qquad (8)$$

The term (ΔP) represents the difference in the pressure across the impingement wall up to the exhaust which has been measured by a differential manometer.

Experimental Method Verification

To verify the present experimental steady state test method of impingement case where IR technique was used to measure the wall temperature, the results of average Nusselts number $(\overline{Nu})$ with (Re_j) werecompared with the test methods given by [8],as shown in figure (6).The wall temperatures were measured using IR technique. Both tests were conducted for the same holes geometry of inline arrangements, number of holes, and $(\frac{H}{D} = 2 \text{and } \frac{H}{D} = 3)$.values. Same trend of$(\overline{Nu})$ variation with (Re_j) was observed, and approximately both dictated same level of $(\overline{Nu})$ values. It is fair to say that the present experimental method is approved to be a reliable method.

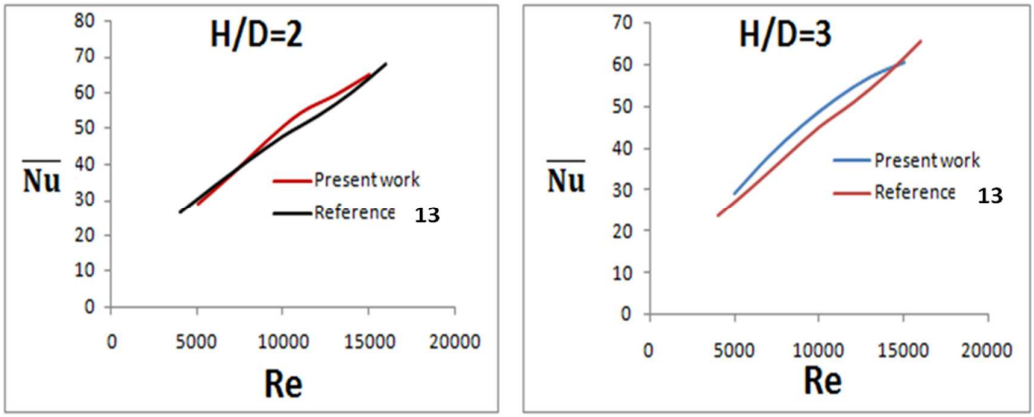

Fig. 6: Experimental verification of (Nu) verses (H/D) with that of (13)

Experimental work

Resultsand Discussion

The flow characteristic of impinging jets for inline arrangements at ($\frac{H}{D} = 2$ and $\frac{H}{D} = 3$). In the present study, the parametric variation of the heat transfer coefficient (Nusselt number) shows an increasing trend with the increase in the Reynolds number for all case. Similarly the Nusselt number can generally be seen to be increasing with the corresponding increase in the Reynolds number, Figure (7)shows the wall cooling effectiveness(η) varaition in spanwise direction model (1) smooth flat plate baseline case at($\frac{H}{D} = 2$and $\frac{H}{D} = 3$), and model (2) triangular ribs at $\left(\frac{H}{D} = 2 \text{ and } \frac{H}{D} = 3\right)$. The wall cooling effectiveness(η) is increased with (X/D) up to (X/D= 32) for all (Re) at$\left(\frac{H}{D} = 2\right)$ and up to (X/D= 28) $\left(\frac{H}{D} = 3\right)$further more wall cooling effectiveness(η) tend to decrease beyond(X/D= 28) at($\frac{H}{D} = 3$). The region laying between (X/D=0) to (X/D=28) shows best wall cooling effectiveness(η) ($\frac{H}{D} = 3$), in which the impingement jets are deflected away towards the downstream direction due to the effect of cross flow induced by upstream jets. The deflection becomes significant as the flow progresses downstream of the first raw as seen in Figure (7). The momentum of the impingement jets is reduced due to the interaction with cross flow, and this affects the rate of heat transfer at stagnation region. This cross flow shows a positive enhancement on heat transfer at the downstream region where high momentum and flow velocity are creating due to jet flow accumulation, and this will enhance the wall effectiveness in the downstream direction.

Figures (8) present the variation of average Nusselts number ($\overline{\text{Nu}}$),Average wall cooling effectiveness($\overline{\eta}$)and discharge coefficient (CD) with Reynolds number respectively, and shows the Nusselts number ($\overline{\text{Nu}}$) increase when Reynolds number(Re) increase for all cases. Figure (9) is represented the temperature distribution of target plate backside for two models baseline and lateral triangular ribs at $\frac{\text{H}}{\text{D}} = 2$ and at$\frac{\text{H}}{\text{D}} = 3$with Re no.between(5000-13000)

Figure (10) shows the experimental jet impact tapping on the clean target and ribbed target plate respectively.

The maximum increments in coefficient of the heat transfer(Nusselt number) and effectiveness of the wall cooling were 32.885%, 22.13% at $\frac{H}{D} = 2$ and 31.37%, 14.58% at $\frac{H}{D} = 3$ respectively.

In this work the effect of the ribs shape, geometry and arrangement are examined and effect jet Reynolds number(R_{ej}) on the average heat transfer coefficient and average wall cooling effectiveness are evaluated for clean and ribbed target surfaces.

Pressure Losses and Discharge Coefficient

The pressure loss is expressed in term of discharge coefficient (C_D), since the pressure drop is a combination of flow contraction in the impingement jet plate and the shear force induced due to friction take places within the cooling passage. Figures (8) show the influence of (H/D) on the discharge coefficient (C_D) for inline array. The result shows a significant influence of H/D on the discharge coefficient or pressure drop for inline array. For inline array, (C_D) is increased as H/D increased indicating a lower pressure drop as (H/D) increased for the same Reynolds number or jets velocity. In low jet distance (H/D), the cross flow passage is narrowed, therefore the flow shear effect is increased leading to low (C_D) values.

Heat Transfer Correlations

The data of cooling performance are presented in terms of Nusselts and Reynolds number. For all (H/D) values, ($\overline{\text{Nu}}$) values are increased with increasing of (Re_j)and maximum heat transfer was obtained at (H/D = 2), for both models. The average Nusselts number of the present tests results can be correlated using the conventional non-dimensional approach that considering the above parameter as follows:

$$\left(\overline{\mathbf{Nu}} = \mathbf{C}\,\mathbf{Re_j^n}(\mathbf{H/D})^{\mathbf{m}}\,\mathbf{pr^v}\right)$$

where, C, n, m and v are constants determined by experiments.

The experimental results were gathered, and the least square mathematical technique was implemented to obtain the following correlation for both smooth target plate and triangular ribs target plate for inline array .

Smooth target plate:

$$\overline{Nu} = 0.0833\, Re_j^{0.711}\, (H/D)^{-0.06875}\, Pr^{0.33} \qquad (9)$$

Square ribs target plate:

$$\overline{Nu} = 0.0804\, Re_j^{0.763} \left(H/D\right)^{-0.183}\, Pr^{0.33} \qquad (10)$$

The maximum deviation between the experimental($\overline{Nu}$) and correlated($\overline{Nu}$) for smooth flat plate and triangular ribbed target plat is 4.83%,7.18 respectively, from range of (Re_j =5000 to 15000).

Conclusions

The heat transfer characteristics and pressure loss have been investigated and the following conclusions can be derived from the present work for impingement cooling system.

1- For clean target plat the heat transfer coefficient (Nusselt number) is increased in the downstream direction (X/D) in the region laying between (X/D=0) to (X/D=28) for all (R_{ej}) at $\frac{H}{D} = 2$.

2- the avarage heat transfer coefficient (Nusselt number) and average wall cooling effectiveness are highly depended upon the jet Reynolds number and ribs arrangement.

3- For lateral Square ribbed target plate the wall cooling effectiveness (η) is increased graduilly with (X/D) and the maximum value of ((Nusselt number)) is occured at (X/D=32) at $\frac{H}{D} = 2$.

4- The average heat transfer coefficient (Nusselt number) and average wall cooling effectiveness are the best for laterial ribs case for all jet Reynolds number and (H/D).

5- The maximum increments in coefficient of the heat transfer(Nusselt number) and effectiveness of the wall cooling were 32.885%, 22.13% at $\frac{H}{D} = 2$ and 31.37%, 14.58% at $\frac{H}{D} = 3$ respectively.

6- From the structure of jet impingement flow field the high level of turbulence is generated with pair of vortex in the space between the triangular ribs and jet spacing.

7- Both jet spacing and Reynolds number have an evident effect on the discharge coefficient. For both cases, low (C_D) values are obtained at jet spacing $\frac{H}{D} = 2$ and high (C_D) at jet spacing $\frac{H}{D} = 3$.

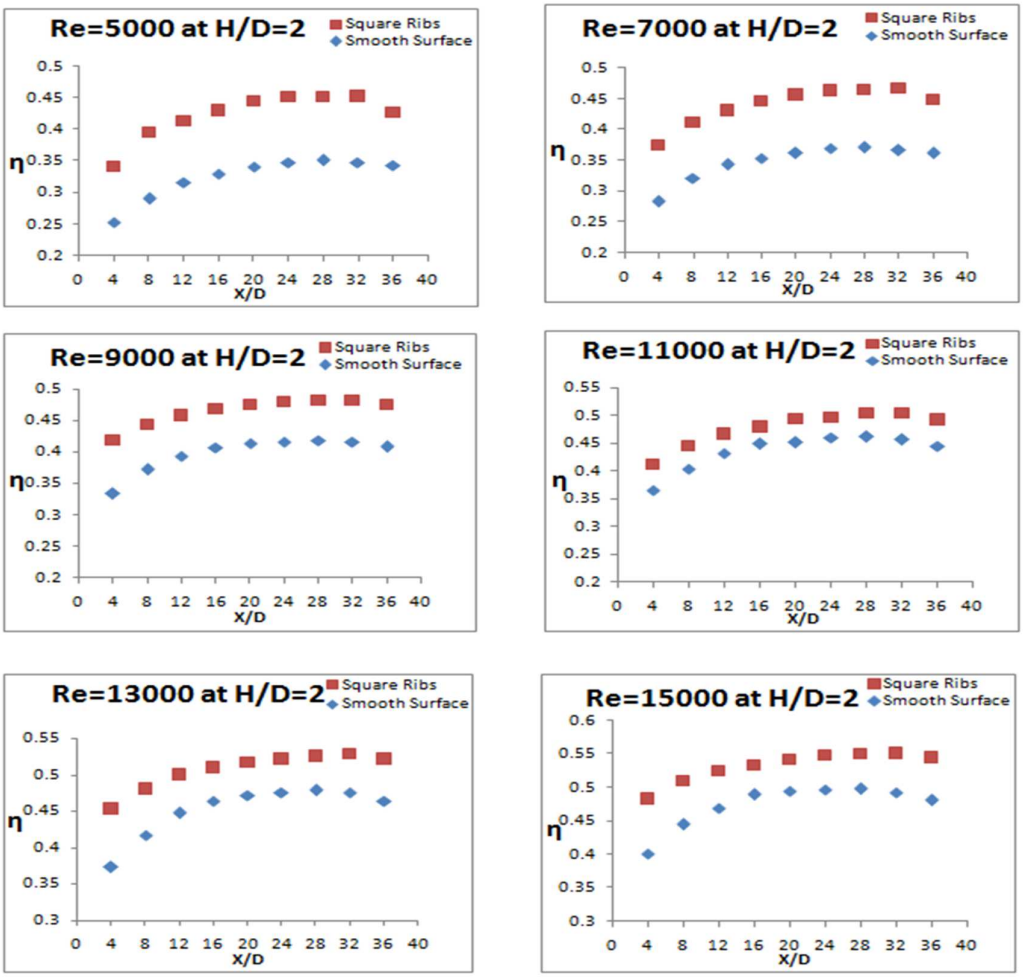

Fig.(7-a): The (η) variation along the downstream direction with different (Re) at (H/D = 2) for square ribs and smooth surface

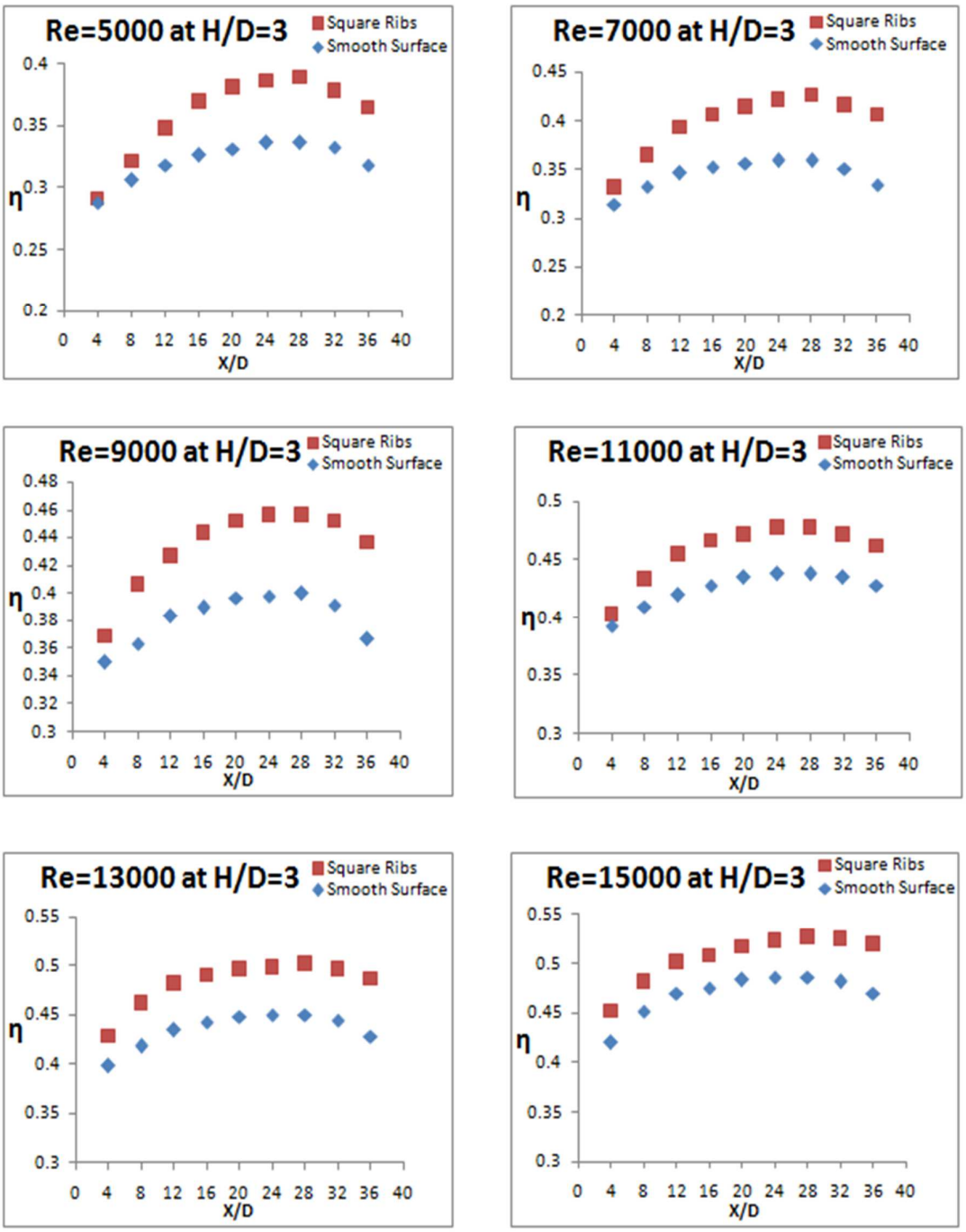

Fig.(7-b): The (η) variation along the downstream direction with different (Re) at $(H/D = 3)$ for square ribs and smooth surface

Fig. 7: The (Nu) variation along the downstream direction with different (Re) : models (1, 2)

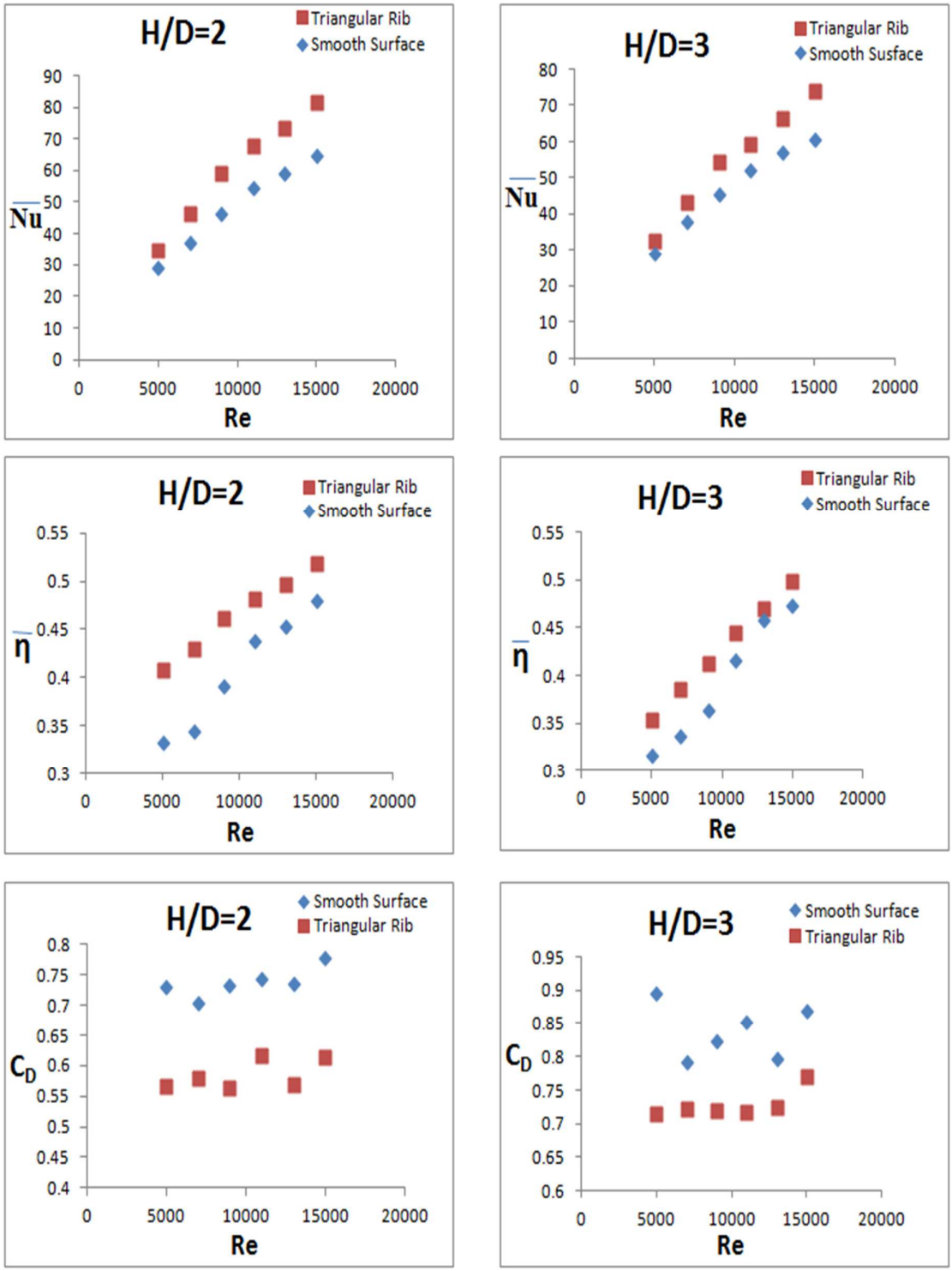

Fig. 8: present the variation of average Nusselts number($\overline{Nu}$), average wall cooling effectiveness ($\overline{\eta}$) and discharge coefficient (C_D) with Reynolds number(Re)

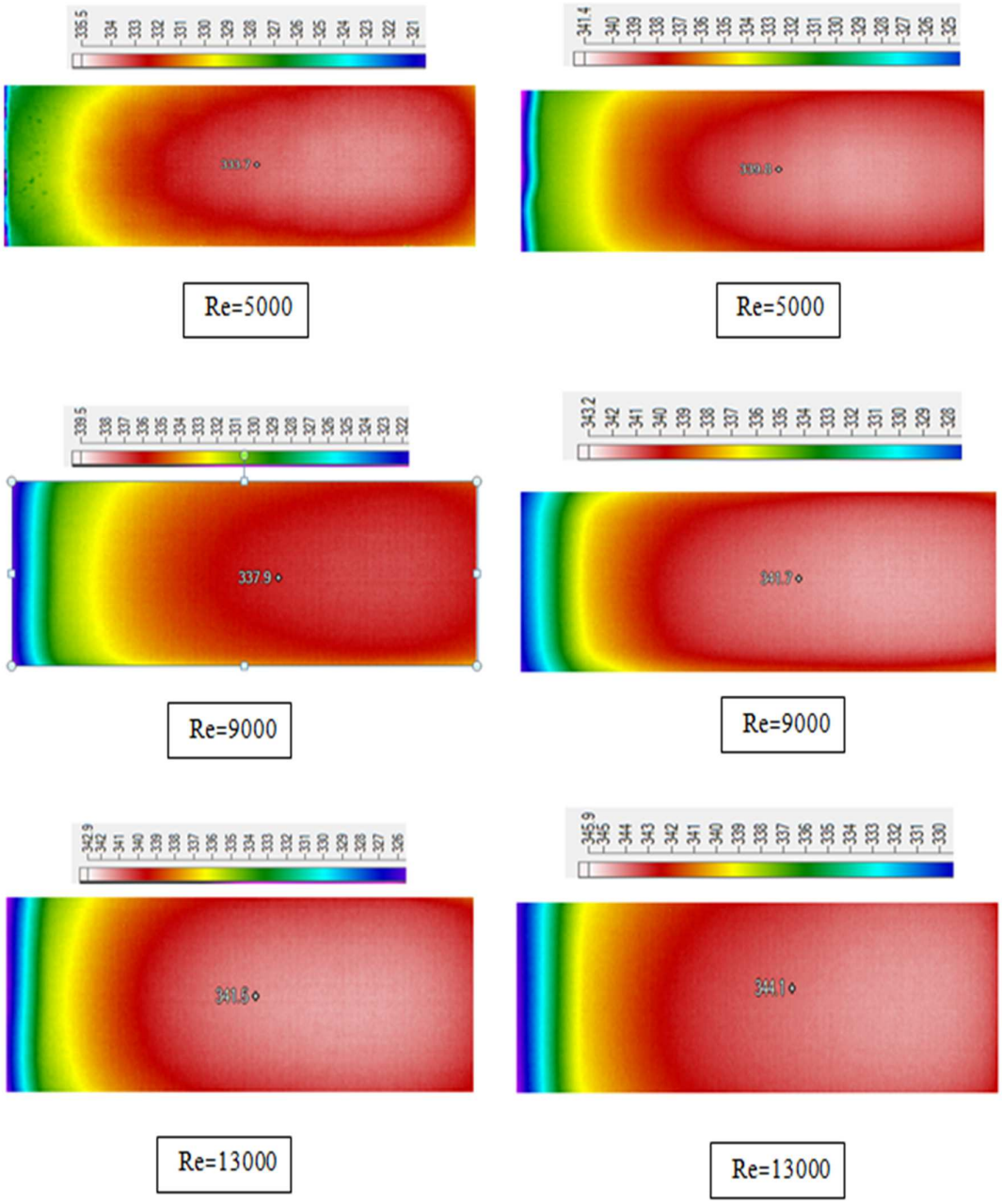

Temperature distribution of target plate backside ($\frac{H}{D}=2$) clean target plate) for Reynolds numbers (5000-13000).	Temperature distribution of target plate backside ($\frac{H}{D}=2$) square ribbed target plate)for Reynolds numbers (5000-13000).

Fig. 9-a: Temperature distribution of target plate backside at ($\frac{H}{D}=2$)

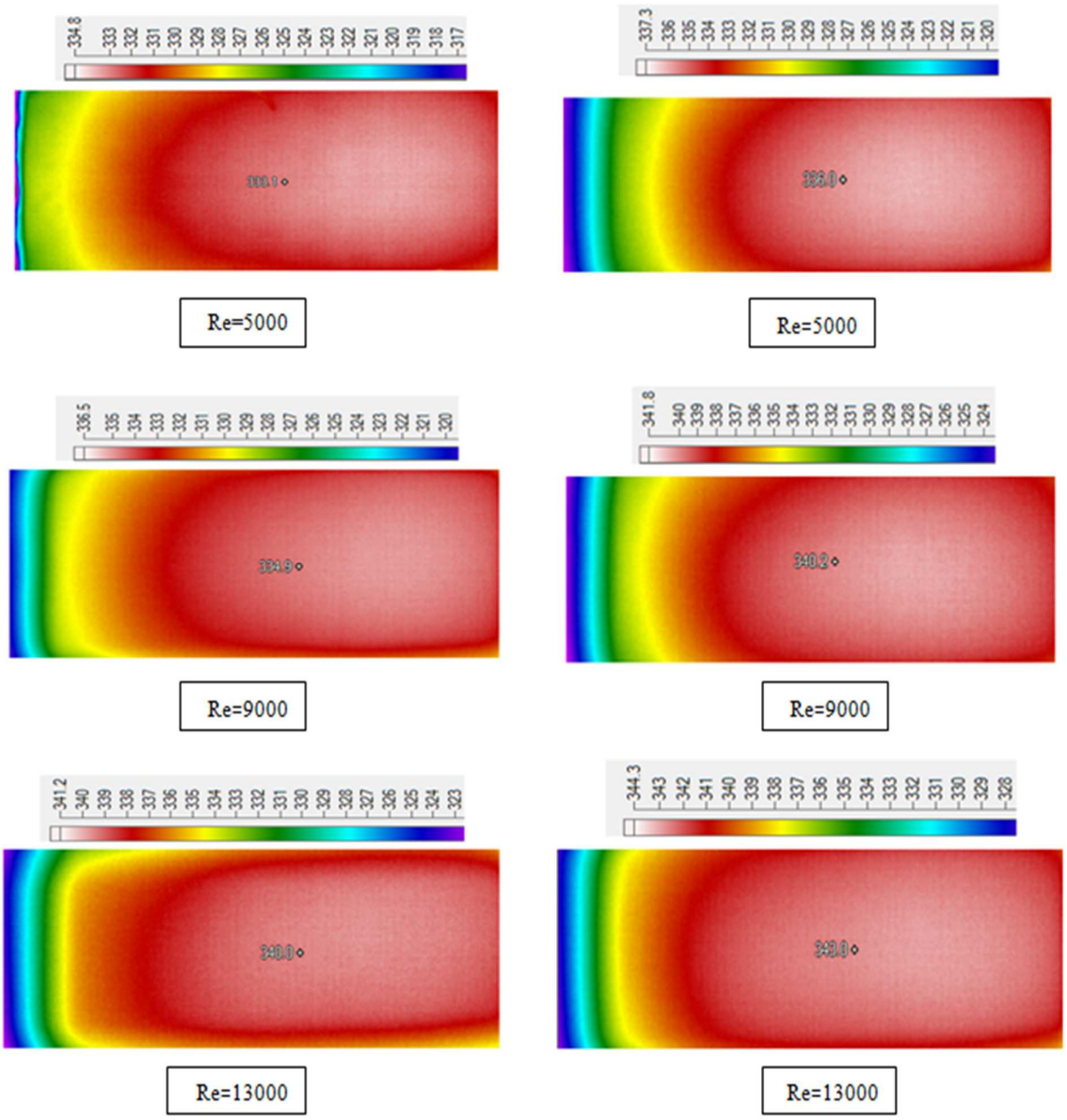

Temperature distribution of target plate backside (3D clean target plate) for Reynolds numbers (5000-13000) .

Temperature distribution of target plate backside (3D square ribbed target plate)for Reynolds numbers (5000-13000).

Fig. 9-b: Temperature distribution of target plate backside at ($\frac{H}{D} = 3$)

Fig. 9: Temperature distribution of target plate backside

Fig. 10-a: Effect of hot jet impact on the clean target plate

Fig. 10-b: Effect of hot jet impact on the square ribbed target plate
Fig. 10: Effect of hot jet impact on two models of target plate

Numerical work

A numerical study is introduced to physically explain the flow characteristics and the phenomena associated with flow field in the jet impingement area. ANSYS FLUENT 14.5 package is used to perform the numerical simulation of the jet impingement system[16]. Three–dimensional model is introduced, second order upwind is selected for discreteness of the governing equations, and standard ($\mathcal{K} - \epsilon$) turbulence model is applied. The air is taken as the working fluid and the flow characteristics are assumed to be steady, Newtonian, incompressible and turbulent. The governing equations, continuity, momentum, and energy for turbulent flow are solved according to [14], [15]. A SOLID WORK PREMIUM 2014 was used to draw the geometry of the experimental model. Unstructured tetrahedron mesh was used to discretize the computational domain into a finite number of control volumes by using the finite–volume scheme. Figure (11) show the mesh of present model for impingement plate. Structured mesh is ruled out because it is favorable for easy cases and it becomes insufficient and time consumed for complicated geometries [16]. The model was meshed by GAMBIT software.

Boundary Conditions:

Both impingement and target plates are regarded as solid boundary surfaces. The volumes of the secondary and mainstream flows are regarded fluid boundary condition. Inlet velocities for both flows are specified. The inlet temperatures for both secondary and mainstream flows are 100 ^{O}C and 40 ^{O}C, respectively, while the inlet velocity of mainstream flow is fixed at 20 m/s and secondary flow velocity is adjusted depending on the Reynolds Number values. Turbulent intensity (TU) for both flows is chosen according to Reynolds Number and mainstream velocity values. The hydraulic diameter for both flows depends on the inlet flow geometry. The outlet domain is specified as pressure outlet for both flows, as shown in the figure (12). The pressure is assumed to be atmospheric for both inlet mainstream and outlet secondary and mainstream flows. To reduce the amount of grids and calculation time, symmetric boundary condition is applied on one side of the geometry.

RESULTS AND DISCUSSION

Flow Feature (computational work):

The behavior of the impinging jets array is described as a very complex behavior because of two reasons which are, the strong deflection at stagnation regions and the strong jet to jet in addition to the jet to crossflow interaction. The deep analysis for the heat transfer rate lead to the correct prediction and understanding mechanism of the flow field. According to the previous researches in the literature that relate with the impingement system, the angle at 90^0 is the optimum angle of the jet that gives the high heat transfer, where the greatest momentum of flow is strike on the target plate [17].

Figure (5-13) shows the impinging jets flow characteristic in inline arrangements when the value of Re = 5000 and $H/D = 2$ in x-y plane. The outcome reveals that the velocity vector colored by temperature within the cooling passage. Also, the deflection of impingement jets can be seen towards the downstream direction because of the influence of crossflow caused by upstream jets. The deflection becomes significant as the flow progresses downstream of the first raw. The momentum of the impingement jets is decreased because of the cross flow interaction as well as the heat transfer rate effect at stagnation area. And when using ribs shows the effect of square rib shape to decrease the crossflow and appears enhancement on the heat transfer. Figure (5-14) viewed the contour temperature distribution on target plate between the mainstream and secondary flows The high temperature can be noticed clearly at ribs arrangement on the impingement area, while the cross flow decrease on this regions. The temperature distribution importance is to provide an indication or appears enhancement of heat transfer distribution at the target plate as well as another indication that relates with the effectiveness of cooling or heating distributions. The cross flow shearing over the surfaces of the rib generates high turbulent level as shown in Figures (5-15) which present the vector of velocity in on the wall target plate. vectors of the predicted velocity for rib model at the difference jets position present obviously the turbulent and the vorticity is greater than that of smooth target surface plate.This figure aid this decision when the model of rib is improved the process of heat transfer.

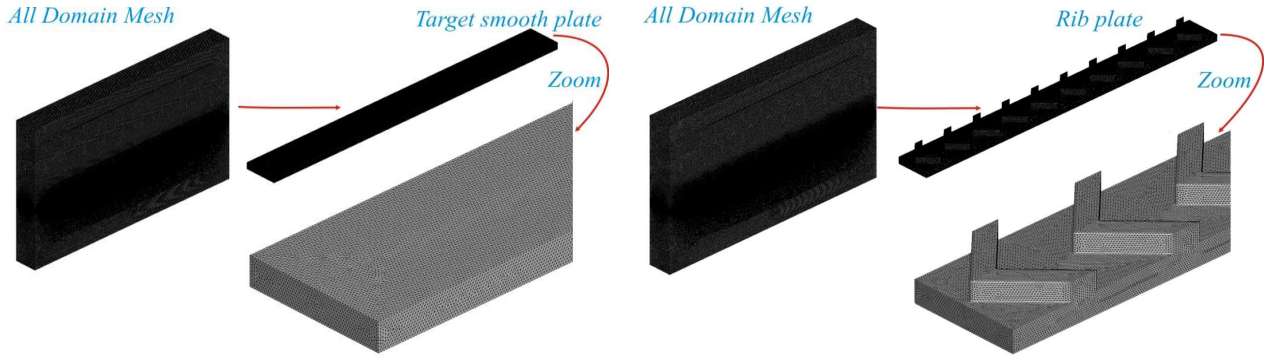

Fig.11: Mesh model

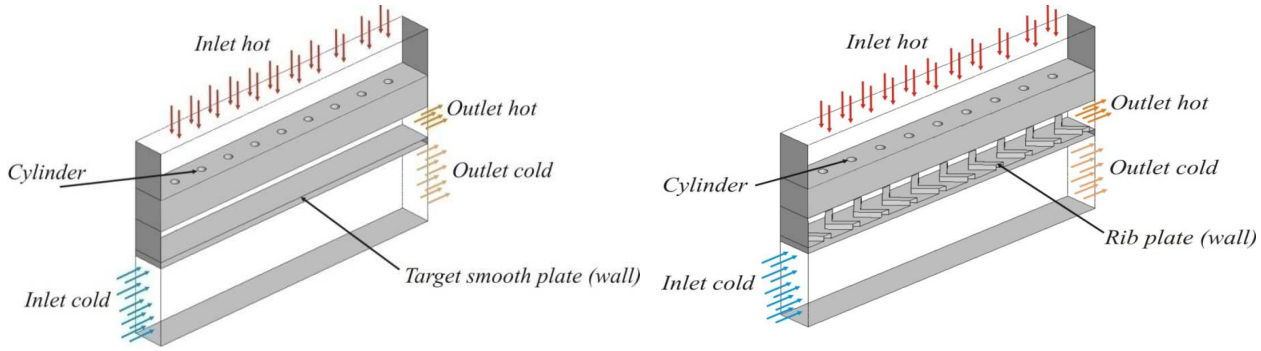

Fig. 12: Schematic structure of impingement cooling system

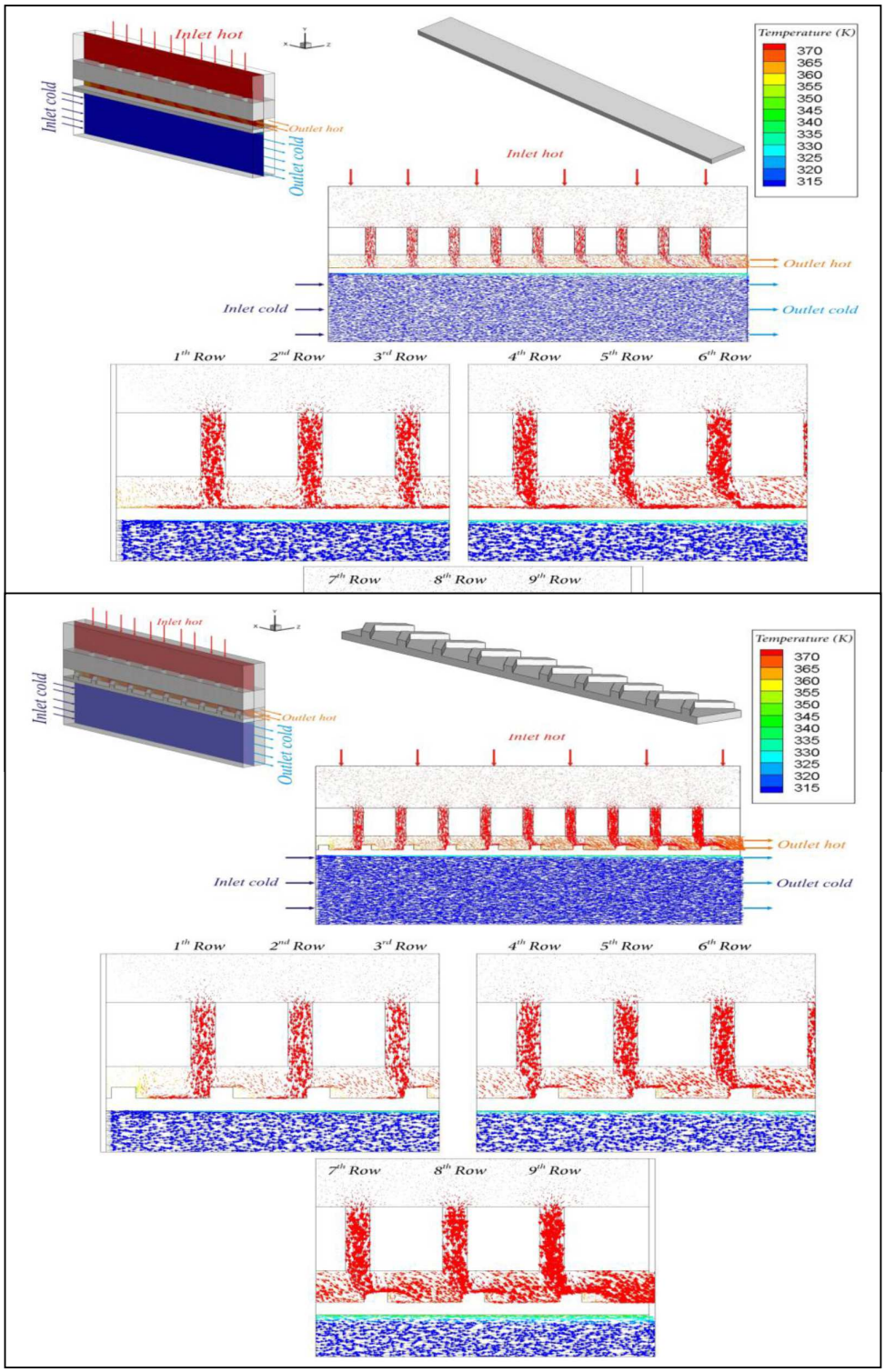

Fig. 5-13: Flow vectors colored by temperature in (x-y) plane for Inline array at (H/D = 2) and (Re = 5000) (smooth flat plate) (square ribbed plate)

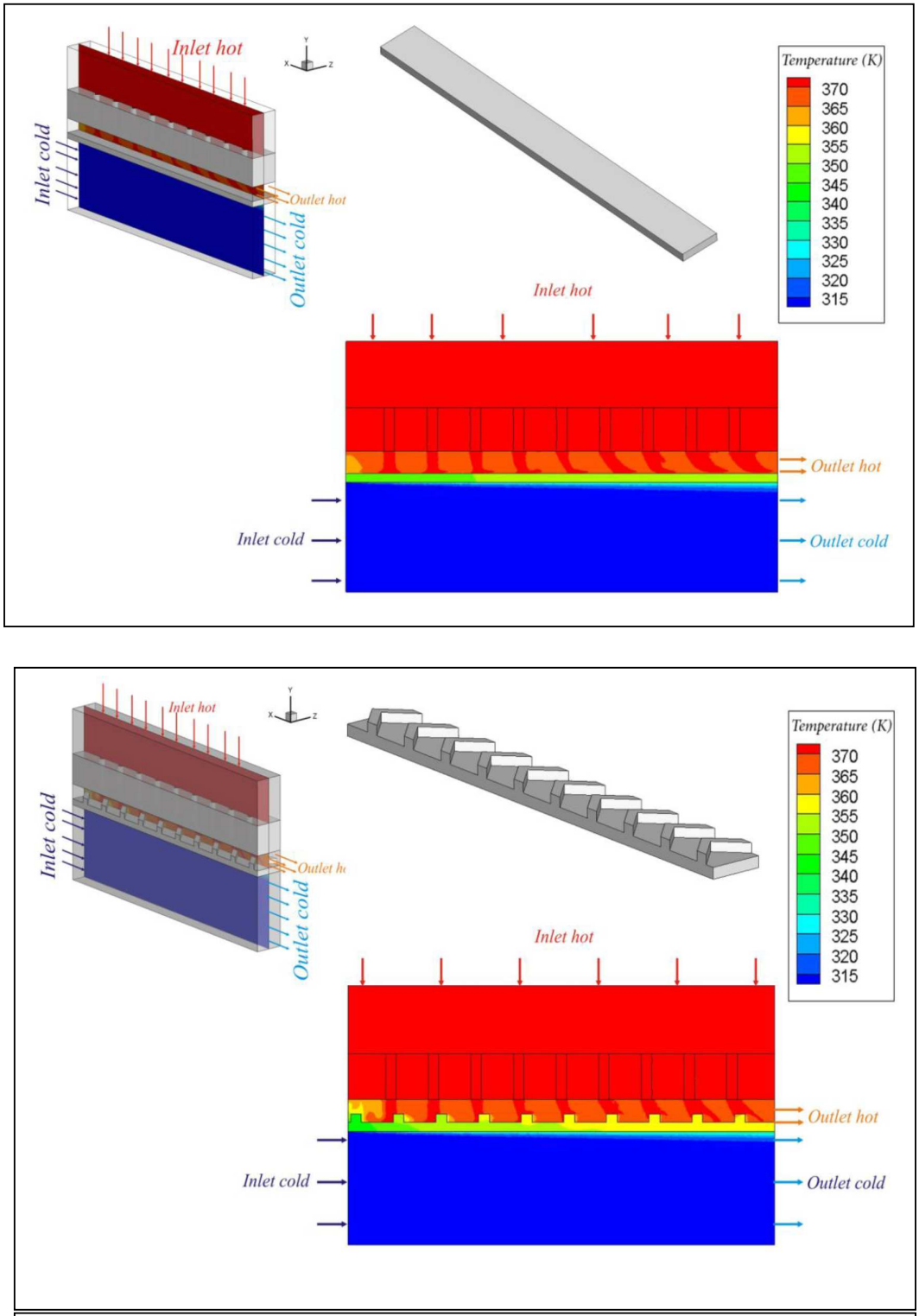

Fig. 5-14: Mainstream and secondary flows contour colored by temperature distribution in (x-y) plane for (square ribbed surface and smooth surface) at (H/D=2) and (Re=5000)

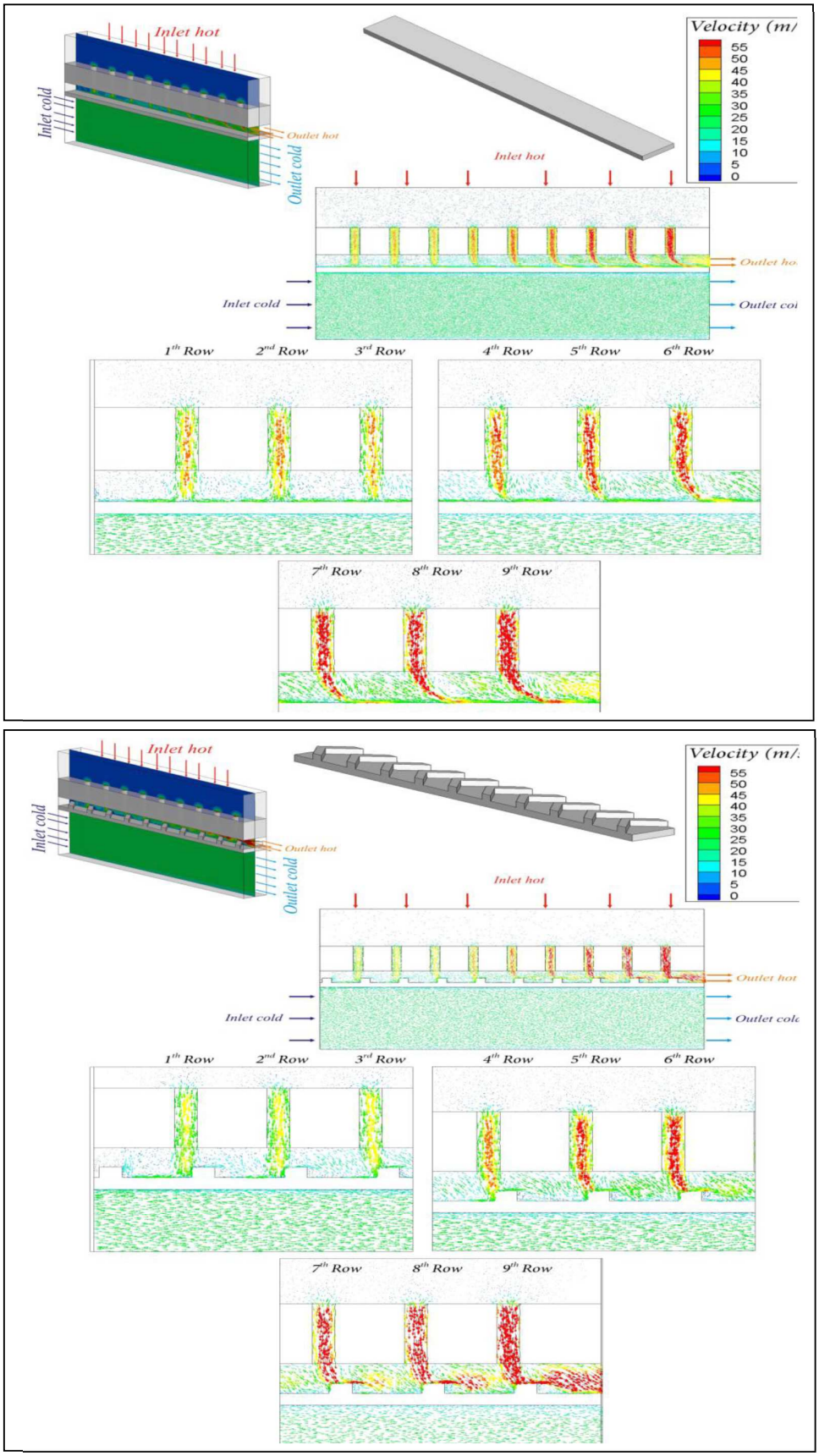

Fig. 5-15: Flow vectors colored by velocity in (x-y) plane for Inline array at (H/D = 2) , (Re = 9000) (smooth surface plate) , (ribbed square target plate)

REFERENCES

1. Dano, Bertrand, et al, 'Flow Characteristics and Heat Transfer Performance of a Semi-Confined Impingement Array of Jet: Effect of Nozzle Geometry, "International Journal of Heat and Mass Transfer Vol. 48, 2005: 691-701.
2. San, Jung-Yang and Mao. De Lai. "Optimum Jet-to-Jet Spacing of Heat Transfer for Staggered Arraysof Impinging Air Jets." International Journal of Heat and Mass Transfer Vol. 44, 2001: 3997 – 4007
3. Cheong, C.Y and Peter Ireland Flow and Heat Transfer Characteristics of an Impinging Jet in Crossflowat Low Nozzle- to- Target Spacing: Part 1. Proc. of the ASME Turbo, June 2005, Reno-Tahoo. Nv.
4. Florschuetz, L.W, D.E. Metzger, and C.C. Su, "Heat Transfer Characteristics for Jet Array Impingement with Initial Crossflow", Journal of Heat transfer Vol. 106, 1984: 34-40.
5. Tabakoff, W. Clevenger, W. 'Gas Turbine Heat Transfer Augmentation by Impingement of Air Jets Having Various Configurationś, ASME, Journal of Engineering for Power, Jan. 1972, pp. 51-60
6. Bailey, J.C. and R.S. Bunker Local Heat Transfer and Flow Distribution for Impinging Jet Arrays ofDense and Sparse Extent. Proc. of the ASME Turbo Expo, June 2002, Amsterdam: Netherlands.
7. Hebert, Ryan, Srinath Ekkad, and Lujai Gao. "Impingement Heat Transfer Part II: Effect of Streamwise Pressure Gradient." Journal of Thermo Physics and Heat Transfer Vol. 18, 2004.
8. Ekkad, S.V. and D.M. Kontrovitz, 'Jet Impingement Heat Transfer on Dimpled Target Surfaces'', International Journal of Heat and Fluid Flow Vol. 23, 2002:22-28
9. Han, J.C., J.S. Park, and C.K. Lei, "Augmented Heat Transfer in Rectangular Channels of Narrow Aspect Ratios with Rib Turbulators. "International Journal of Heat and Mass Transfer Vol. 32, 1989:1619-1630.
10. Hebert, Ryan, Srinath Ekkad, and Lujai Gao. "Impingement Heat Transfer Part II: Effect of Streamwise Pressure Gradient." Journal of Thermo Physics and Heat Transfer Vol. 18, 2004.
11. Andrews, G.E., Hussain, C.I., and Ojobor, S.N. "Full Coverage Impingement Heat Transfer. I. Chem. E.,Symposium Series No 86, 1985 and Text Book on Impingement Heat Transfer: 2008
12. Hollworth, B.R. and Barry, R.D. "Heat Transfer from Array of Impinging Jets with Large Jet-to-JetSpacing, ASME, Paper No. 78 – GT-117.
13. Bayer A. K., "Experimental investigation of jet impingement cooling on ribbed target surface", Msc. thesis, University of Technology, Baghdad,(2015).
14. Versteeg H. K. and Malalasekera W., (1996), "An introduction to computational fluid dynamics the finite volume method", Longman Group, London.
15. Roy D. N., (1987), "Applied fluid mechanics", Affiliated East-West Private LTD, New Delhi.
16. "Fluent 14.5 use، guide, programing and tutorial guide", Fluent, Version 14.5, Ansys Inc., 2009.
17. Lamyaa A. E. and Deborah A.K., " Experimental investigation of local heat transfer distribution on smooth and roughened surfaces under an array of angled impinging ", ASME Journal of Turbomachinery, Vol.127, pp. 590-597, 2005